HHS Public Access

Author manuscript

Free Radic Biol Med. Author manuscript; available in PMC 2020 June 01.

Published in final edited form as:

Free Radic Biol Med. 2019 June ; 137: 37–45. doi:10.1016/j.freeradbiomed.2019.04.013.

Upstream Signaling Events Leading to Elevated Production of Pro-Survival Nitric Oxide in Photodynamically-Challenged Glioblastoma Cells

Jonathan M. Fahey[a], **Witold Korytowski**[b], and **Albert W. Girotti**[a,*]

[a]Department of Biochemistry, Medical College of Wisconsin, Milwaukee, WI, 53226-3548

[b]Department of Biophysics, Jagiellonian University, Krakow, Poland

Abstract

Nitric oxide (NO) generated endogenously by inducible nitric oxide synthase (iNOS) promotes growth and migration/invasion of glioblastoma cells and also fosters resistance to chemotherapy and ionizing radiotherapy. Our recent studies revealed that glioblastoma cell iNOS/NO also opposes the cytotoxic effects of non-ionizing photodynamic therapy (PDT), and moreover stimulates growth/migration aggressiveness of surviving cells. These negative responses, which depended on PI3K/Akt/NF-κB activation, were strongly suppressed by blocking iNOS transcription with JQ1, a BET bromodomain inhibitor. In the present study, we sought to identify additional molecular events that precede iNOS transcriptional upregulation. Akt activation, iNOS induction, and viability loss in PDT-challenged glioblastoma U87 cells were all strongly inhibited by added L-histidine, consistent with primary involvement of photogenerated singlet oxygen ($^1O_2$). Transacetylase p300 not only underwent greater Akt-dependent activation after PDT, but greater interaction with NF-κB subunit p65, which in turn exhibited greater K310 acetylation. In addition, PDT promoted intramolecular disulfide formation and inactivation of tumor suppressor PTEN, thereby favoring Akt and p300 activation leading to iNOS upregulation. Importantly, deacetylase Sirt1 was down-regulated by PDT stress, consistent with the observed increase in p65-acK310 level, which fostered iNOS transcription. This study provides new mechanistic insights into how glioblastoma tumors can exploit iNOS/NO to not only resist PDT, but to attain a more aggressive survival phenotype.

Keywords

Photodynamic Therapy; Glioblastoma; Oxidative Stress; Nitric Oxide; Inducible Nitric Oxide Synthase; Stress Signaling

[*]To whom correspondence should be addressed: *Prof. Albert W. Girotti, Ph.D., Department of Biochemistry, Medical College of Wisconsin, Milwaukee, WI, 53226-3548, Tel: 414-955-8432, Fax: 414-955-6510, agirotti@mcw.edu.*

1. Introduction

It is well established that many tumors generate nitric oxide (NO) in relatively low fluxes to promote cell growth, angiogenesis, and migration/invasion [1-4]. Such NO, which derives mainly from inducible nitric oxide synthase (iNOS/NOS2), can also play a key role in tumor resistance to chemotherapy, radiotherapy, and also pro-tumor immunosuppression [5-10]. iNOS is subject to upregulation in response to various stresses experienced by tumor cells, e.g. stresses arising from vascular deficiencies [1-3]. At high steady state levels (e.g. >500 nM generated by inflammatory macrophages), NO is typically cytotoxic. Cytotoxicity may be manifested via reaction of NO with superoxide to give highly oxidizing peroxynitrite or direct reaction with iron-sulfur proteins, thereby inactivating them [3]. However, at relatively low levels (e.g. 50-300 nM in tumors), NO can activate pro-survival/expansion signaling pathways by modifying effector proteins such as EGFR, Ras, Src, HIF-1α, and PI3K-dependent Akt [11,12]. Modification typically occurs via S-nitrosation (SNO formation) of specific cysteine residues with lower than normal pK_a values [13,14]. However, the S-nitrosating agent is usually not NO itself, but rather an oxidized derivative such as nitrous anhydride (N_2O_3) [14]. SNO-mediated NO signaling can be difficult to assess because SNO groups are not particularly stable and can be deleted after signaling pressure subsides, e.g. by the thioredoxin or glutaredoxin systems [15].

Photodynamic therapy (PDT) was introduced in the mid-1970s as an innovative approach for selectively eradicating various solid tumors in cancer patients [16-19]. In 1996, Photofrin®-based PDT was the first such modality to receive FDA approval for clinical use [16]. PDT is a minimally invasive approach involving (i) systemic or topical application of a photosensitizing agent (PS) or metabolic precursor, (ii) PS photoexcitation by non-ionizing radiation, typically light in the far visible to near-infrared wavelength range, and (iii) molecular oxygen [16,17]. Reactive oxygen species (ROS) such as singlet oxygen ($^1O_2$) are produced, which damage PS-accessed sites, i.e. tumor cells per se or surrounding vascular cells [17,20]. Light-independent side effects of PDT are usually negligible, and cytotoxicity is usually limited to the tumor site at which light is delivered, typically via fiber optic transmitters. The administered PS can either be a pre-existing agent such as Photofrin® [16-20] or a pro-sensitizer such as 5-aminolevulinic acid (ALA) [21,22]. Upon entering a target cell, ALA is metabolized to the functional PS, protoporphyrin IX (PpIX), via the heme biosynthetic pathway, PpIX accumulating initially in mitochondria [22]. This pathway is significantly stimulated in most rapidly growing tumor cells, and elevated PpIX levels under iron-limiting conditions increase target specificity and phototoxicity for this type of PDT.

Early studies by others using mouse syngeneic tumor models revealed that NO from an unidentified NOS isoform(s) significantly reduced Photofrin®-PDT effectiveness [23,24]. This was mainly attributed to effects on the tumor microvasculature, i.e. vasodilation by NO opposing vasoconstriction by PDT [24]. More recent studies in the authors' laboratory revealed that iNOS-derived NO in various ALA/light-challenged human cancer lines (breast, prostate, glioblastoma) signaled for (i) greater resistance to apoptotic photokilling and (ii) greater proliferative and migratory aggressiveness in cells that survived the challenge [25-32]. More often than not, these effects were attributable to photostress-upregulated

iNOS/NO, which also occurred in mouse-borne breast tumor xenografts after ALA-PDT [33]. We showed recently that iNOS transcription in glioblastoma cells is NF-κB-dependent and mediated by interaction of bromodomain protein Brd4 with acetylated K310 on the p65 subunit of NF-κB [34]. Blocking iNOS transcription with a Brd4-binding BET bromodomain inhibitor (JQ1) was found to be much more effective in limiting NO's anti-PDT effects than using inhibitors of iNOS enzymatic activity [34].

In the present study, we sought a better understanding of the upstream signaling mechanisms that lead to greater p65 acetylation, iNOS/NO upregulation, and hyper-resistance/aggressiveness in glioblastoma cells after an ALA/light challenge. Glioblastomas are highly aggressive and lethal brain malignancies which typically persist after surgical resection, chemotherapy or radiotherapy [35,36]. PDT has emerged as a promising new alternative treatment for these difficult tumors [37-40] Our findings in this study may suggest novel strategies for improving PDT efficacy against glioblastoma and possibly other solid malignancies as well.

2. Materials and methods

2.1. General materials

Sigma-Aldrich (St. Louis, MO) supplied the 5-aminolevulinic acid (ALA), H_2O_2, L-histidine, L-alanine, N-ethylmaleimide (NEM), fetal bovine serum (FBS), growth media, antibiotics (penicillin, streptomycin), and other cell culture materials were from. GlaxoSmithKline, LLC (Research Triangle Park, NC) provided the iNOS inhibitor GW274150 via material transfer agreement. Cayman Chemicals (Ann Arbor, MI) supplied the iNOS inhibitor 1400W (N-[3-aminomethyl)benzyl] acetamidine), NO scavenger cPTIO (2-(4-carboxyphenyl)-4,4,5,5-tetramethylimidazoline-1-oxyl-3-oxide), PI3K inhibitor LY294002, p300 acetyltransferase inhibitor C646, and a rabbit polyclonal antibody against human iNOS. Rabbit monoclonal antibodies against human p-Akt (Ser-473), total Akt, p-PI3K (Tyr-199/Tyr-458), total PI3K, p-p300 (Ser-1834), total p-300, p65, Sirt1, Sirt2, and β-actin were from Cell Signaling Technologies (Danvers, MA). Abcam (Cambridge, MA) supplied the rabbit polyclonal antibody against p65-acK310. Peroxidase-conjugated IgG secondary antibodies and control IgG were from Cell Signaling Technologies.

2.2. Cell culture conditions

Human glioblastoma U87-MG cells were obtained from and authenticated by the American Type Culture Collection (ATCC), Manassas, VA. From here on, these cells are referred to as simply U87. The cells were cultured in minimal essential medium (MEM) with Earle's salts supplemented with 10% FBS, 1% pyruvate, penicillin (100 units/ml) and streptomycin (0.1 mg/ml). Culture dishes were kept in a humidified incubator at 37 °C under 5% CO_2. Proliferating cells were switched to fresh growth medium every third day and were passaged fewer than six times for all experiments described.

2.3. Cell sensitization and irradiation

U87 cells at 60-65% confluency in 35-mm transparent culture dishes were cleared of growth medium and then metabolically sensitized with PpIX by incubating with 1 mM ALA in

serum-free and phenol red-free MEM for 30 min in the dark. ALA-induced PpIX at this point was located mainly in mitochondria, as demonstrated previously [22]. The medium was then removed and replaced with fresh MEM without ALA/serum/phenol red. For some dishes, 1 mM or 3 mM L-histidine or L-alanine was included in the MEM and kept at the same starting concentration throughout. After an additional 15 min of dark incubation, all dishes (those without L-His or L-Arg, and those containing either one) were placed on a translucent plastic platform over a bank of four 40W cool-white fluorescent lamps and irradiated at 25 °C. Light fluence rate (irradiance) at the inside bottom of each 35-mm dish was ~11 W/m^2, as measured with a YSI radiometer (Yellow Springs, OH). Irradiation time was usually 15 min, corresponding to a total light dose (fluence) of ~1 J/cm^2. In some instances, an iNOS activity inhibitor (1400W or GW274150), NO scavenger (cPTIO), PI3K inhibitor (LY294002), or p300 inhibitor (C646) was introduced immediately after irradiation and maintained at the same concentration from there on. After various post-irradiation times, cell samples were collected for determination of residual viability and surviving cell proliferation and invasion rates. Cells exposed to ALA-alone or light-alone were analyzed alongside as dark or light controls, respectively, for the PDT experiments. (For this *in vitro* study, the term PDT is defined as “photodynamic treatment” and is distinguished from PDT as “photodynamic therapy”, which should be reserved for the clinical procedure.)

2.4. Examination of PTEN oxidation status after a PDT challenge

U87 cells at 60% confluency were sensitized with ALA-induced PpIX as described in the preceding section. After cells were switched to ALA/serum/phenol red-free medium, they were exposed to a 1 J/cm^2 light fluence. L-Histidine (3 mM) was added to some cells prior to irradiation to check for any $^1O_2$-mediated PTEN photooxidation; control cells received L-alanine at the same starting concentration. After irradiation, the cell medium was aspirated and replaced with 10% FBS-containing medium without or with L-His or L-Ala. At selected post-irradiation incubation times, non-oxidized thiol groups were blocked by treating cells with 20 mM NEM in lysing medium [20 mM Tris-Cl buffer (pH 7.4), 150 mM NaCl, 5% glycerol, 0.1% Nonidet-P40 detergent, and protease inhibitor mixture], followed by sonication and centrifugation [41]. Some cells served as positive controls by incubation with the known PTEN oxidant, H_2O_2 (e.g. 250 μM for 2 h), followed by lysis-NEM treatment, sonication and centrifugation. Supernatant fractions recovered after centrifugation were analyzed for total protein content by BCA assay, and then subjected to Western blotting under non-reducing conditions. Other details were as described by Zhang *et al.* [41].

2.5. Western blot procedures

The expression of total iNOS, PI3K, Akt, PTEN, p300, p65-ack310, Sirt1, and Sirt2 in U87 cells before and after a PDT challenge was assessed by Western immunoblotting, as was the phosphorylation-activation status of PI3K (p-PI3K), Akt (p-Akt), and p300 (p-p300). Irradiated cells, along with controls, were recovered from dishes by gentle scraping, centrifuged, and washed with cold PBS. All cells, except those intended for PTEN analysis (see Sect. 2.4), were suspended in cold pH 7.4 lysis buffer containing protease inhibitors and homogenized as described previously [25-29]. After centrifugation, the supernatant fractions were analyzed for total protein content, after which samples were separated by SDS-PAGE using appropriate proportions of acrylamide/bis-acrylamide and reducing conditions, except

for PTEN [41]. Separated proteins were transferred to a polyvinylidene difluoride membrane. After blocking, the membrane was treated overnight at 4 °C with a given antibody, using a supplier-recommended dilution from a stock solution. After washing, the membrane was treated with a peroxidase-conjugated IgG secondary antibody, after which protein bands were detected using SuperSignal West Pico-PLUS-based chemiluminescence (Thermo Scientific, Rockford, IL).

2.6. Detection of p300 interaction with p65

The possibility that PDT-enhanced acetylation of p65-K310, as observed previously [34], is facilitated by greater physical interaction of p300 with NF-κB/p65 was examined using an immunoprecipitation approach. After ALA/light treatment, U87 cells were switched to 10% FBS-medium and returned to the incubator for 6 h, after which they were lysed and total lysate protein determined. Dark control cells (ALA-only) were prepared alongside. A sample of p300 monoclonal antibody (10 μl from a 1:100 diluted stock solution) was added to 250 μg of cell lysate and incubated for 16 h at 4 °C with slow agitation. A 100 μl aliquot of a protein A-conjugated Sepharose bead slurry was then added to each lysate, followed by 6 h of additional incubation at 4 °C with agitation. Non-specific IgG served as a control. After centrifugation, the beads with attached proteins were washed three times with lysis buffer to remove any contaminating proteins, then treated with 50 μl of pH 2.6 glycine buffer (0.2 M) to release remaining proteins. After centrifugation, proteins were recovered in supernatant fractions, which were brought to pH 8.0 using 20 mM Tris-Cl buffer. Samples were then subjected to SDS-PAGE, followed by immunoblotting for p65 and p300. Total lysates were analyzed alongside. Reverse-order immunoprecipitation was also carried out in which p65 was used to pull down p300 in ALA/light-treated samples *vs.* dark controls.

2.7. Assessment of cytotoxicity and surviving cell proliferation

The cytotoxic effects of ALA/light on U87 cells (viability loss) over a 24 h post-irradiation period were assessed by CCK-8 assay, using a live cell counting kit from Dojindo Molecular Technologies (Rockville, MD) and a 96-well plate reader for A_{540} measurements. Cells treated with an iNOS inhibitor (1400W) or NO trap (cPTIO) immediately after irradiation were analyzed alongside, as were ALA-only or light-only controls. All cell counts were expressed relative to starting values. Twenty-four hours after the PDT challenge, proliferation rate of cells that could withstand the challenge was monitored as follows. After a wash to remove detached (dead or dying cells), remaining live cells, along with non-irradiated controls, were overlaid with 10% FBS-containing medium and proliferation rate over an additional 24-36 h of dark incubation in the absence *vs.* presence of 1400W or cPTIO was assessed, using the CCK-8 assay.

2.8. Assessment of surviving cell invasiveness

A 96-place Trans-well device (Model MBA96) from NeuroProbe (Gaithersburg, MD) was used for examining the invasiveness of U87 cells that survived an ALA/light challenge. Immediately after irradiation, these cells were switched to serum-free medium and, along with dark (ALA-only) controls, were treated with various inhibitors, e.g. LY294002, C646, GW274150 or cPTIO, then transferred to the upper wells of the invasion chamber (225 μl per well). Before this, 10% FBS-containing medium (225 μl) was placed in each lower well

of the chamber, the serum serving as a cell attractant. A Matrigel-infused polycarbonate filter with 8-μm pores was attached over each lower well. After a pre-warming period (37 °C for ~30 min), the upper and lower wells were clamped together, and the entire device was placed in the incubator. Twenty-four hours later, the upper well media, along with cells that had not traversed the filters, were carefully removed. Invasive cells that had traversed were detached by centrifugation into 10% FBS-medium, transferred to a 96-well plate, and quantified by CCK assay. Other details were as described previously [31-34].

2.9. Statistical evaluations

Graphical data are presented as means ± SE of values from at least 3 replicate experiments. The two-tailed Student's *t*-test in conjunction with GraphPad Prism software was used for determining the statistical significance of perceived differences between experimental values. P values <0.05 were considered statistically significant.

3. Results

3.5. iNOS/NO-mediated pro-survival responses in glioblastoma cells after a PDT challenge

We determined first whether an ALA/light oxidative challenge might provoke pro-survival responses in U87 cells and if so, whether iNOS-derived NO played a role in these responses. As shown in Fig. 1, the viable fraction of ALA-treated cells decreased progressively after exposure to a 1 J/cm^2 light fluence, reaching ~0.7 after 24 h of dark incubation. When 1400W, a specific iNOS inhibitor, was present from the outset, the viability loss after 24 h was significantly greater by ~25 %. In consistent fashion, the NO scavenger cPTIO boosted the viability loss at 24 h by ~32% relative to control (Fig. 1). Each of these findings, in agreement with previous ones [32,32], suggested that iNOS/NO was acting cytoprotectively via one or more signaling pathway(s). When viable cell count was tracked beyond the 24 h post-irradiation point, we observed a steady increase over the next 48 h, which reflected surviving cell proliferation. However, the surviving ALA/light-treated cells grew significantly more rapidly than dark (ALA-only) controls, the rate from 24-48 h post-irradiation being ~60% greater (Fig. 1). Importantly, 1400W and cPTIO each reduced the elevated rate to near background level, implying that iNOS/NO played an important role in the pro-growth aggressiveness of surviving cells. This confirmed our previous observations on these and other cancer cell types, and set the stage for characterizing the responsible stress signaling [31-34].

3.2. Upstream determinants of iNOS overexpression in photodynamically-stressed cells.

We showed previously that iNOS underwent a rapid and prolonged upregulation in glioblastoma U87 and U251 cells after a moderately cytotoxic ALA/light challenge [32,34]. ALA-induced PpIX is often described as a Type II photosensitizer, i.e. one acting via the formation of singlet oxygen ($^1O_2$), a highly reactive ROS [42,43]. The imidazole group of the natural amino acid, L-histidine (L-His), is known to react rapidly with $^1O_2$, the rate constant being ~2×10^8 $M^{-1}s^{-1}$ in water [44]. Because of its potent $^1O_2$ scavenging ability, L-His is often used as a preliminary *in vitro* diagnostic for $^1O_2$ involvement in photodynamic reactions [45,46]. To learn whether $^1O_2$ played a role in photostress

upregulation of iNOS in U87 cells, we irradiated them in the presence of 3 mM L-His. The latter was introduced after ALA pre-incubation to eliminate the possibility it might somehow alter PpIX generation. L-Alanine (L-Ala), which does not scavenge $^1O_2$ at any appreciable rate [44], was used as a control. As shown by the Western blot in Fig. 2A, U87 cells sensitized with ALA-induced PpIX exhibited a striking upregulation of iNOS after irradiation in the presence of 3 mM L-Ala, the level attained at 6 h post-hv being nearly 4-times that of the non-irradiated control (ALA alone). A control without L-Ala exhibited approximately the same boost in iNOS level (not shown) with an eventual drop-off, as reported previously [34]. Added L-His strongly reduced the post-hv iNOS induction (~70% decrease at 6 h) (Fig. 2A), suggesting that $^1O_2$ was the initial stimulating oxidant in the induction process. As observed previously [32,34], the cytoprotective and pro-growth effects of iNOS/NO such as described in Fig. 1 were more likely dependent on stress-upregulated enzyme than on pre-existing enzyme. It is reasonable to assume that the pro-growth signaling program set in motion by elevated iNOS/NO [29-34] was still in operation after the iNOS had declined, e.g. >24 h after irradiation (Fig. 2).

Not unexpectedly, $^1O_2$ played a key role in the cytotoxic effects of PDT, which were opposed by iNOS/NO's cytoprotective effects (Fig. 1). As shown in Fig. S1, the viability of U87 cells 24 h after PDT was reduced by ~35% relative to non-irradiated controls. Whereas 3 mM L-Ala had no significant protective effect, 3 mM L-His decreased the viability loss to ~10%, consistent with scavenging/inactivation of $^1O_2$.

3.3. PI3K and Akt activation as early pro-survival events in PDT-challenged cells.

The PI3K/Akt signaling pathway plays a central role in cancer cell survival and proliferation in many types of malignancies [47-50]. Upon stimulation of an upstream modulator (receptor tyrosine kinase or G-protein-coupled receptor), class-I phosphatidylinositol 3-kinases (PI3Ks) become phosphorylation-activated, leading to conversion of membrane phosphatidylinositol-4,5-diphosphate (PIP_2) to phosphatidylisositol-3,4,5-triphosphate (PIP_3) [49,50]. PIP_3 accumulation in the plasma membrane promotes recruitment of phosphatidylinositol-dependent kinase-1 (PDK1) and serine/threonine protein kinase Akt/PKB, resulting in phosphorylation-activation of the latter with increased cell survival/expansion [47-50]. In many different human cancers, PI3Ks exhibit activity-enhancing mutations in their p110α subunits [49,50]. Although effects of PDT on Akt status were examined in our previous studies using breast cancer and glioblastoma cell lines [28,34], PI3K status was not similarly monitored. As shown by the Western blot in Fig. 3A, overall PI3K expression in U87 cells was not affected by ALA/light treatment. On the other hand, the level of phosphorylation-activated PI3K (p-PI3K) increased rapidly after a PDT challenge in the presence of added L-Ala (3 mM), reaching an apparent maximum at ~15 min after irradiation and then declining during continued incubation (Fig. 3A). The increase in p-PI3K was strongly blunted by L-His (3 mM), suggesting that $^1O_2$ played a major role in this early upstream post-PDT event.

We showed previously that the potent tumor-promoting kinase Akt was rapidly phosphorylation-activated in U87 cells after a moderately cytotoxic ALA/light challenge. As shown by the Western blot in Fig. 3B, the level of p-Akt rose substantially in control cells

with added L-Ala during post-irradiation dark incubation, reaching nearly 7-times that of non-irradiated (dark control) cells after 6 h, whereas overall Akt remained unchanged. These cells exhibited essentially the same rise in p-Akt as cells lacking the L-Ala (not shown), indicating that the amino acid had no unexpected effects. Elevated p-Akt returned to nearly its basal level after 22 h, as observed previously [34]. When L-His was present during irradiation, the rise in p-Akt was strongly attenuated, reaching only ~40% of the level observed in L-Ala controls after 3 h and 6 h (Fig. 3B). Thus, $^1O_2$ appeared to play a major role in the activation of Akt as well as PI3K under photooxidative stress.

In previous studies, we found that a PI3K inhibitor prevented both Akt photo-activation and iNOS upregulation in two different cancer cell lines [28,34]. These findings, along with the results in Figs. 2 and 3, suggest the following generalized course of events for photostressed U87 cells: (i) $^1O_2$-provoked PI3K activation, resulting in higher PIP_3 levels, (ii) greater Akt activation catalyzed by PDK1 and possibly also mTORC2 [51], (iii) activation and nuclear translocation of transcription factor NF-κB, (iv) increased iNOS expression.

3.4. Inactivation of PTEN in response to photooxidative stress

By catalyzing the de-phosphorylation of PIP_3 to PIP_2, the cytosolic enzyme PTEN (phosphatase and tensin homolog) plays a major role in the negative regulation of PI3K/Akt, and thus acts as a potent tumor suppressor [52-54]. When exposed to an oxidant like H_2O_2, PTEN can undergo rapid inactivation via -S-S- bond formation between Cys residues 71 and 124 [55]. We asked whether this might be occurring in photostressed U87 cells, thereby causing stimulation of the PI3K/Akt pathway. As shown by the Western blot in Fig. S2, which was prepared under typical reducing conditions, PTEN in ALA/hv-treated U87 cells appeared as a single band (M_r ~54 kDa), the intensity of which remained constant relative to a dark control over a 24 h period of post-hv incubation. When cell lysates were analyzed under non-reducing conditions, a dark control exhibited PTEN mainly as the single band observed under reducing conditions, whereas for irradiated cells, a more rapidly migrating band representative of the oxidized (-S-S-) form was observed (Fig. 3C). When L-His was present during irradiation, much less of the oxidized PTEN was present (Fig. 3C), which is consistent with $^1O_2$ involvement in PTEN oxidation. However, a direct attack of $^1O_2$ itself on PTEN was unlikely because the $^1O_2$ would have originated in mitochondria (where PpIX photosensitization occurred) and its short lifetime [44,45] would have precluded any significant reaction with cytosolic PTEN. Until additional mechanistic information is acquired, one can speculate that the actual oxidant was a relatively mobile and long-lived $^1O_2$ adduct such as a mitochondrial lipid hydroperoxide [56].

3.5. Activation of p300 in response to photooxidative stress

The acetyltransferase p300 and its paralog CREB-binding protein (CBP) act as transcriptional co-activators for several tumor-promoting transcription factors [57,58]. p300/CBP stimulates gene expression at promoter sites by catalyzing acetylation of key lysine residues on histones as well as transcription factors such as NF-κB [59,60]. Studies on TNF-κ-stimulated lung carcinoma cells revealed that p300-mediated acetylation of lysine-310 (acK310) on the p65/RelA subunit of NF-κB allowed p65 to be recognized by another co-activator, bromodomain-containing protein 4 (Brd4) [61,62]. The latter acted as

an epigenetic “reader” of p65-acK310, thereby fostering transcription at NF-κB promoter sites. Although not examined in those studies [61,62], p300 may have been activated via Akt-mediated phosphorylation of Ser-1834, as demonstrated earlier by another group [63]. Accordingly, we assessed the effects of photodynamic stress on the p300 status of glioblastoma U87 cells. As shown in Fig. 4A, the overall p300 protein level in ALA/light-treated cells remained unchanged relative to a dark control over a 24 h post-hv period. However, the level of Ser-1834-phosphorylated p300 (p-p300) increased progressively during post-irradiation incubation, reaching >3-times the control level after 6 h and slowly declining thereafter (Fig. 4B). The PI3K inhibitor LY294002 prevented the strong post-irradiation increase in p-p300 (Fig. 4C), suggesting that PI3K-dependent Akt was the responsible kinase, in agreement with previous observations on TNF-α-treated lung cancer cells [62].

To probe further into the upstream mechanism of iNOS induction in ALA/light-challenged U87 cells, we monitored p65-acK310 status at various post-irradiation times. As shown by the Western blot in Fig. 5A, the level of p65-acK310 increased progressively during post-hv incubation, reaching more than 3-times the dark control level by 24 h. Most of the cells (>90%) were still attached at this point. We recently reported a similar upregulation of p65-acK310 for photostressed U87 cells [34]; however, we did not probe into underlying mechanism [34]. When the PI3K inhibitor LY294002 was introduced immediately after irradiation, p65-acK310 remained at or near the control level throughout (Fig. 5B), indicating that PI3K/Akt played a crucial upstream driving role. Similar results were obtained when the p300 activity inhibitor, C646, was present (Fig. 5C), indicating that p-p300 was also necessary for the photostress upregulation of p65-acK310. D646 had no significant effect on progressively greater p-p300 formation after ALA/hv treatment (Fig. S3; compare with Fig. 4B), confirming that D646 inhibited p-p300 activity, but not p-p300 formation itself. These findings are consistent with those of other investigators using different stimulatory agents (e.g. cytokines) and different cancer cells [63].

Importantly, iNOS upregulation under photostress, like p65-acK310 upregulation, was found to be greatly attenuated by C646 (Fig. 2B; compare with Fig. 2A). This, along with previous evidence [34], clearly supports the idea that transcriptional over-expression of iNOS was directly dependent on greater p65-acK310 formation.

3.6. Interaction of p300 and p65 in photodynamically challenged cells

Using a pull-down approach in a previous study [34], we showed that physical contact between transcriptional co-activator Brd4 and NF-κB p65 existed in U87 cells, and this was markedly enhanced after a photodynamic challenge. That response was underscored by a dramatic upregulation of Brd4 protein [34]. We asked in the present study whether a similar photostress-enhanced association between p300 and p65 might occur in conjunction with PI3K/Akt/p300/NF-κB activation leading ultimately to iNOS upregulation. To investigate this, we used a pull-down procedure in which overall U87 p300 was immunoprecipitated before and after an ALA/light challenge, collected on protein A-linked Sepharose beads, then released and checked for p65 inclusion by immunoblotting. As shown in Fig. 6A, the p300 immunoprecipitate revealed a clear p65 immunoblot band which was more intense for

photostressed cells, indicating greater p65-p300 association after cells were photochallenged. As expected, immunoblotted p300 in the immunoprecipitates remained constant throughout, as did immunoblotted p65 and p300 in the total lysates (Fig. 6A). To corroborate the results shown in Fig. 6A, we carried out a reverse-order pulldown in which a p65 immunoprecipitate was analyzed for amount of associated p300. In non-stressed U87 control cells, a clear p300 immunoblot band was observed (Fig. 6B). After ALA/light treatment, the intensity of this band was much greater (Fig. 6B), signifying greater p65-p30 association in photostressed cells and consistent with our results based on p300 pull-down (Fig. 6A). Although this was not specifically examined, the stress-enhanced p65-p300 interaction is likely to have occurred in the nucleus, where p300 may have pre-existed and p65 translocated after NF-κB activation [34].

3.7. Down-regulation of Sirt1 in ALA/light-challenged cells

Sirtuins are NAD^+-dependent Class-III histone deacetylases (HDACs) that modulate gene expression via removal of acetyl groups on histones and non-histone substrates [64]. Sirt1, the most widely studied mammalian sirtuin, is best known for its ability to deacetylate non-histone proteins such as p53 and NF-κB p65 [65-67]. In a seminal early study involving lung epithelial cells, it was found that Sirt1 inhibited NF-κB transcription by catalyzing p65 deacetylation at lysine-310, thereby sensitizing the cells to TNF-α-induced apoptosis [67]. Based on this information and the fact that the p65-acK310 level in U87 cells was elevated after PDT stress, we asked how this elevation might be reflected in Sirt1 status. To address this, we tracked Sirt1 protein level as a function of post-irradiation time. As shown in Fig. 7A, Sirt1 protein (M_r ~110 kDa) underwent a progressive decline after photodynamic challenge, reaching ~20% of the dark control level by 24 h. In sharp contrast, the expression of another Class-III histone deacetylase, Sirt2 (M_r ~39 kDa), remained unchanged throughout a 21 h post-hv period (Fig. 7B). The relatively weak Sirt1 control band in Fig. 7A suggests a certain degree of constitutive downregulation of this enzyme to explain the observed pre-existing p65-acK310 (Fig. 5). The photostress-induced upregulation of p65-acK310 (Fig. 5A) compared with down-regulation of Sirt1 (Fig. 7A) demonstrates a strikingly well-coordinated pro-survival signaling system in which iNOS/NO upregulation ultimately plays a key role. It is not known at present whether Sirt1 down-regulation was an early response to a primary oxidant like $^1O_2$ or whether it occurred secondarily, e.g. to PI3K/Akt activation.

3.8. Role of PI3K/Akt/p300 activation and iNOS induction in hyper-invasiveness of PDT-stressed glioblastoma cells

Having shown that the PI3K/Akt/p300/p65-acK310 network lies upstream of pro-survival/pro-growth iNOS induction after PDT (Fig. 1), we asked whether activation of this network might stimulate cell migration/invasiveness. Assessing this was important because iNOS/NO is known to play a key signaling role in glioblastoma cell migration/invasion as well as proliferation [4,68,69]. Invasion measurements were started immediately after irradiation of ALA-primed cells, using a 96-place trans-well device with Matrigel-infused filters. Various inhibitors or a NO scavenger were introduced at the outset and maintained at the indicated starting concentrations throughout. Non-irradiated controls (ALA-only) were monitored alongside. As shown in Fig. 8, PI3K inhibitor LY294002 and p300 inhibitor C646 each

reduced constitutive U87 invasion by a small (yet insignificant) extent relative to the non-treated control, whereas NO trap cPTIO, and iNOS inhibitor GW274150 had no obvious effect in this basal state. Consistent with earlier findings [34], cells that withstood a PDT (ALA/light) challenge, and remained viable after 24 h, invaded more rapidly than dark controls by a significant 30% (Fig. 8). Importantly, LY294002 and C646 each eliminated this rate increase, reducing invasiveness to the control level, while GW274150 and C646 lowered the increase significantly. It is clear from these findings that photostress activation of the PI3K/Akt/p300/p65/iNOS network was a key driving force behind accelerated U87 cell migration/invasion.

4. Discussion

In previous work [32,34], we found that PDT (ALA/light)-stimulated growth and migration/invasion of glioblastoma cells was significantly driven by iNOS induced by the photooxidative stress. In seeking to abrogate or at least minimize these negative effects, we found that inhibitors of iNOS activity or an NO scavenger performed well, but that an inhibitor of BET protein-mediated iNOS transcription was much more effective in this regard. The latter inhibitor (JQ1) acted by preventing a BET protein (Brd4) from binding to acetylated lysine 310 (acK310) on the p65 subunit of transcription factor NF-κB [34]. This inhibition was especially important because in addition to iNOS, these cells exhibited a striking increase in Brd4 and acK310 levels after a photodynamic challenge [34]. Based on our evidence with inhibitors of enzymatic activity and protein transcription [32,34], it was clear that iNOS/NO not only played a major role in cell resistance to photokilling, but also hyper-aggressiveness of surviving cells. We found, however, that other NF-κB-regulated proteins (e.g. Survivin, Bcl-xL, MMP-9) probably contributed to these post-PDT responses because, like iNOS, each of these proteins was upregulated by PDT in JQ1-inhibitable fashion [34]. Although JQ1 may have suppressed Survivin, Bcl-xL, and MMP-9 transcription, an indirect effect via iNOS suppression was also possible, since NO is known to signal for induction of these effector proteins [3,7,8]. Consequently, iNOS/NO appeared to be an overarching downstream driver of PDT-enhanced cell survival and expansion. Having demonstrated these negative downstream responses and how they might be attenuated, we turned our attention to early upstream events in the present study.

One of the very earliest events to occur would have been ROS generation following photoexcitation of ALA-induced PpIX. We used exogenous L-histidine to test whether singlet oxygen ($^1O_2$) might be a primary ROS, knowing that the imidazole group of this amino acid quenches $^1O_2$ at a high rate, $1.0–1.5 \times 10^8$ $M^{-1}s^{-1}$ [44]. Relatively high histidine concentrations were used (up to 3 mM), realizing that the $^1O_2$ lifetime in cells is very short [42,45] and that sufficient histidine would have to be internalized and reach mitochondria, where most of the PpIX was localized [32]. In addition to strongly blunting iNOS upregulation, exogenous histidine inhibited PDT-induced upstream phosphorylation-activation of PI3K and Akt, and oxidative inactivation of PTEN (intramolecular -S-S- formation). By contrast, L-alanine, a relatively weak $^1O_2$ quencher ($k_q \sim 3 \times 10^3$ $M^{-1}s^{-1}$ [44]), had little, if any, effect on the above responses. Although comparing effects of histidine *vs.* alanine is not conclusive with regard to $^1O_2$ intermediacy, our evidence is at least consistent with this, and numerous photobiological studies have used this approach.

An intriguing question regarding PI3K and Akt activation, and PTEN inactivation, is the identity of the responsible oxidant(s). Singlet oxygen would have been generated in the vicinity of the mitochondrial membrane(s) because PpIX is amphiphilic and our prior evidence indicated that PpIX fluorescence of ALA-treated U87 cells was localized in mitochondria [32]. Since $^1O_2$ reacts rapidly with proximal proteins and unsaturated lipids [45], its lifetime would have been too short for any significant reaction with PTEN, for example, in the cytosol. We speculate, therefore, that $^1O_2$-generated oxidants of much longer lifetimes were responsible. Such oxidants could have been hydroperoxides of mitochondrial membrane lipids (LOOHs). Although phospholipid hydroperoxides might qualify, cholesterol hydroperoxides would be better candidates due to their greater membrane departure rates, higher mobility, and greater resistance to enzymatic reduction [56]. The cholesterol content of cancer cell mitochondrial membranes is also relatively high [70]. It remains to be seen whether such an indirect, LOOH-based mechanism exist, but if so, it would be the first of this type to be demonstrated.

Although we have described phosphorylation-activation of Akt for other cancer lines subjected to Ala/light treatment, our evidence for this in the present study, as well as for PI3K and p300 activation, along with PTEN oxidative inactivation, is novel for glioblastoma cells. It is important to point out that Tsai *et al.* [71] recently reported that p300 is also activated in human melanoma A375 cells after an ALA/light challenge, and that this results in upregulation of cytoprotective cyclooxygenase-2 (COX-2). However, whether this response depended on PI3K/Akt activation was not determined, nor was iNOS status examined after PDT treatment. We recently showed that iNOS-derived NO can stimulate COX-2 expression in PDT-stressed prostate cancer PC3 cells [72]. iNOS/NO might have played a role in the COX-2 upregulation described for A375 cells [71], but this possibility was not assessed by those investigators.

We observed a striking consistency and co-operativity of post-PDT upstream events leading to downstream iNOS upregulation. For example, PTEN inactivation via intramolecular disulfide formation would have favored PI3K activation by increasing PIP_3 availability, which, in turn, would have stimulated Akt activation and thence p300 activation. This evidence is consistent with that of others using different cancer lines and non-PDT stressing [61,63]. In regard to co-operativity, it is particularly interesting that pull-down assays showed a PDT-enhanced interaction of transacetylase p300 and subunit p65 of NF-κB. This, along with a striking downregulation of deacetylase Sirt1, would have fostered acetylation of p65-K310, which is known to be a recognition site for bromodomain protein Brd4, an epigenetic “reader” [62,62]. In previous work [34], we showed that Brd4 and p65-acK310 levels in U87 cells rose substantially after PDT and, furthermore, that Brd4 interacted more extensively with p65. Taken together, these earlier [34] and present observations are consistent with a well-orchestrated stress signaling network leading to an iNOS/NO-mediated pro-survival/expansion outcome. This network, along with postulated LOOH-mediated $^1O_2$ effects, is depicted schematically in Fig. 9.

5. Conclusions

We describe PDT-aggravated growth and invasive aggressiveness of glioblastoma cells in which iNOS/NO plays a major driving role. A chain of upstream effector proteins has been identified, several of which can be pharmacologically suppressed. This suggests novel approaches for inhibiting iNOS/NO antagonistic effects at their earliest stages of development. Glioblastoma is one of the deadliest of human malignancies and ALA-based PDT is known to be one of the most promising therapies for combatting it [73]. Consequently, improving the clinical efficacy of anti-glioblastoma PDT through pharmacologic suppression of iNOS/NO would appear feasible based on our findings.

Supplementary Material

Refer to Web version on PubMed Central for supplementary material.

Acknowledgements

This work was supported by the following grants: NIH/NCI Grant CA70823, Grant 5520347 from the Advancing a Healthier Wisconsin Research and Education Program, and BSC Grant 3308239-FP12605 from the MCW Cancer Center (to A.W.G.); and NCN grant 2017/27/B/NZ5/02620 (to W.K.). The authors thank Dr. Brian C Smith for providing the human Sirt1 and Sirt2 antibodies along with a sample of recombinant human Sirt1. We also thank Jerzy Bazak and Chuanwu Xia for their assistance in finalizing the figures.

References

[1]. Jenkins DC, Charles IG, Thomsen LL, Moss DW, Holmes LS, Baylis SA et al., Roles of nitric oxide in tumor growth. Proc. Natl. Acad. Sci. USA. 92 (1995) 4392–4396. [PubMed: 7538668]

[2]. Fukumura D, Jain RK, Role of nitric oxide in angiogenesis and microcirculation in tumors. Cancer Metastasis Rev. 17 (1998) 77–89. [PubMed: 9544424]

[3]. Burke AJ, Sullivan FJ, Giles FJ, Glynn SA, The yin and yang of nitric oxide in cancer progression. Carcinogenesis 34 (2013) 503–512. [PubMed: 23354310]

[4]. Tran AN, Boyd NH, Walker K, Hjelmeland AB, NOS expression and NO function in glioma and implications for patient therapies. Antioxid. Redox Signal. 26 (2017) 986–999. [PubMed: 27411305]

[5]. Xie QW, Kashiwabara Y, Nathan C, Role of transcription factor NF-kappa B/Rel in induction of nitric oxide synthase. J. Biol. Chem 269 (1994) 4705–4708. [PubMed: 7508926]

[6]. Crowell JA, Steele VE, Sigman CC, Fay JR. Is inducible nitric oxide synthase a target for chemoprevention? Mol. Cancer Ther 2 (2003) 815–823. [PubMed: 12939472]

[7]. Kostourou V, Cartwright JE, Johnstone AP, Boult JKR, Cullis ER, Whitley GSJ, Robinson SP, The role of tumour-derived iNOS in tumor progression and angiogenesis. Br. J. Cancer 104 (2011) 83–90. [PubMed: 21139581]

[8]. Vannini F, Kashfi K, Nath N, The dual role of iNOS in cancer. Redox Biol. 6 (2015) 334–343. [PubMed: 26335399]

[9]. Fionda C, Abruzzesem MP, Santoni A, Cippitelli M, Immunoregulatory and effector activities of nitric oxide and reactive nitrogen species in cancer. Curr Med Chem. 23 (2016) 2618–2636. [PubMed: 27464520]

[10]. Ekmekcioglu, Grimm EA, Roszik J, Targeting iNOS to increase efficacy of immunotherapies. Hum Vaccin Immunother. 13 (2017) 1105–1108. [PubMed: 28121247]

[11]. Thomas DD, Ridnour LA, Isenberg JS, Flores-Santana W, Switzer CH, Donzelli S et al. The chemical biology of nitric oxide: implications in cellular signaling. Free Radic Biol Med. 45 (2008) 18–31. [PubMed: 18439435]

[12]. Switzer CH, Glynn SA, Ridnour LA, Cheng RY, Vitek MP, Ambs S, et al. Nitric oxide and protein phosphatase 2A provide novel therapeutic opportunities in ER-negative breast cancer. Trends Pharmacol Sci. 32 (2011) 644–651. [PubMed: 21893353]

[13]. Thomas DD, Jord'heuil D, S-nitrosation: current concepts and new developments, Antiox Redox Signal. 17 (2012) 924–936.

[14]. Hogg N, Broniowska KA, The chemical biology of S-nitrosothiols, Antiox Redox Signal. 17 (2017) 969–980.

[15]. Sengupta R, Ryter SW, Zuckerbraun BS, Tzeng E, Billiar TR, Stoyanovsky DA, Thioredoxin catalyzes the denitrosation of low-molecular mass and protein S-nitrosothiols. Biochemistry. 46 (2007) 8472–8483. [PubMed: 17580965]

[16]. Dougherty TJ, Gomer CJ, Henderson BW, Jori G, Kessel D, Korbelik M, Moan J, Peng Q, Photodynamic Therapy. J. Natl. Cancer Inst 90 (1998) 889–905. [PubMed: 9637138]

[17]. Agostinis P, Berg K, Cengel KA, Foster TH, Girotti AW, Gollnick SO et al. Photodynamic therapy of cancer: an update. CA Cancer J. Clin 61 (2011) 250–281. [PubMed: 21617154]

[18]. Whelan HT, High-grade glioma/glioblastoma multiforme: is there a role for photodynamic therapy? J. Natl. Compr. Canc. Netw 10 (2012) S31–S34. [PubMed: 23055212]

[19]. Quirk BJ, Brandal G, Donlon S, Vera JC, Mang TS, Foy AB et al. Photodynamic therapy (PDT) for malignant brain tumors--where do we stand? Photodiagnosis Photodyn. Ther 12 (2015) 530–544. [PubMed: 25960361]

[20]. Benov L, Photodynamic therapy: current status and future directions. Med. Princ. Pract 24 (2015) 14–28. [PubMed: 24820409]

[21]. Kennedy JC, Pottier RH, Endogenous protoporphyrin IX, a clinically useful photosensitizer for photodynamic therapy, J. Photochem. Photobiol. B, 14 (1992) 275–292. [PubMed: 1403373]

[22]. Peng Q, Berg K, Moan J, Kongshaug M, Nesland JM, 5-Aminolevulinic acid-based photodynamic therapy: principles and experimental research, Photochem. Photobiol. 65 (1997) 235–251. [PubMed: 9066303]

[23]. Henderson BW, Sitnik-Busch TM, Vaughan LA, Potentiation of photodynamic therapy antitumor activity in mice by nitric oxide synthase inhibition is fluence rate dependent, Photochem Photobiol. 70 (1999) 64–71. [PubMed: 10420844]

[24]. Korbelik M, Parkins CS, Shibuya H, Cecic I, Stratford MR, Chaplin DJ, Nitric oxide production by tumour tissue: impact on the response to photodynamic therapy. Br J Cancer. 82 (2000) 1835–1843. [PubMed: 10839299]

[25]. Bhowmick R, Girotti AW, Signaling events in apoptotic photokilling of 5-aminolevulinic acid treated tumor cells: inhibitory effects of nitric oxide. Free Radic Biol Med. 47 (2009) 731–740. [PubMed: 19524035]

[26]. Bhowmick R, Girotti AW, Cytoprotective induction of nitric oxide synthase in a cellular model of 5-aminolevulinic acid-based photodynamic therapy. Free Radic Biol Med. 48 (2010) 1296–1301. [PubMed: 20138143]

[27]. Bhowmick R, Girotti AW, Rapid upregulation of cytoprotective nitric oxide in breast tumor cells subjected to a photodynamic therapy-like oxidative challenge. Photochem Photobiol. 87 (2011) 378–386. [PubMed: 21143607]

[28]. Bhowmick R, Girotti AW, Cytoprotective signaling associated with nitric oxide upregulation in tumor cells subjected to photodynamic therapy-like oxidative stress. Free Radic Biol Med. 57 (2013) 39–48. [PubMed: 23261943]

[29]. Bhowmick R, Girotti AW, Pro-survival and pro-growth effects of stress-induced nitric oxide in a prostate cancer photodynamic therapy model. Cancer Lett. 343 (2014) 115–122. [PubMed: 24080338]

[30]. Girotti AW, Tumor-generated nitric oxide as an antagonist of photodynamic therapy. Photochem Photobiol Sci. 14 (2015) 1425–1432. [PubMed: 25706541]

[31]. Fahey JM, Girotti AW, Accelerated migration and invasion of prostate cancer cells after a photodynamic therapy-like challenge: Role of nitric oxide. Nitric Oxide. 49 (2015) 47–55. [PubMed: 26068242]

[32]. Fahey JM, Emmer JV, Korytowski W, Hogg N, Girotti AW, Antagonistic effects of endogenous nitric oxide in a glioblastoma photodynamic therapy model. Photochem Photobiol 92 (2016) 842–853. [PubMed: 27608331]

[33]. Fahey JM, Girotti AW, Nitric oxide-mediated resistance to photodynamic therapy in a human breast tumor xenograft model: improved outcome with NOS2 inhibitors. Nitric Oxide. 62 (2017) 52–61. [PubMed: 28007662]

[34]. Fahey JM, Stancill S, Smith BC, Girotti AW, Nitric oxide antagonism to glioblastoma photodynamic therapy and mitigation thereof by BET bromodomain inhibitor JQ1, J. Biol. Chem 293 (2018) 5345–5359. [PubMed: 29440272]

[35]. Behin A, Hoang-Xuan K, Carpentier AF, Delattre JY, Primary brain tumours in adults, Lancet 361(2003) 323–331. [PubMed: 12559880]

[36]. Wen PY, Kesari S, Malignant gliomas in adults, New Engl. J. Med 359 (2008) 492–507. [PubMed: 18669428]

[37]. Whelan HT, High-grade glioma/glioblastoma multiforme: is there a role for photodynamic therapy? J. Natl. Compr. Canc .Netw 10 (2012) S31–S34. [PubMed: 23055212]

[38]. Quirk BJ, Brandal G, Donlon S, Vera JC, Mang TS, Foy AB et al. Photodynamic therapy (PDT) for brain tumors: where do we stand? Photodiagnosis Photodyn. Ther 12 (2015) 530–544. [PubMed: 25960361]

[39]. Bechet D, Mordon SR, Guillemin F, Barberi-Heyob MA, Photodynamic therapy of malignant brain tumors: a complementary approach to conventional therapies, Cancer Treat. Rev 40 (2014) 229–241. [PubMed: 22858248]

[40]. Olzowy B, Hundt CS, Stocker S, Bise K, Reulen HJ, Stummer W, Photoirradiation therapy of experimental malignant glioma with 5-aminolevulinic acid, J. Neurosurg 97 (2002) 970–976. [PubMed: 12405389]

[41]. Zhang Y, Han SJ, Park I, Kim I, Chay KO, Kim SM, et al. Redox Regulation of the Tumor Suppressor PTEN by hydrogen peroxide and tert-butyl hydroperoxide, Int. J Mol Sci 18 (2017) 982; doi: 10.3390/ijms18050982.

[42]. Foote CS, Mechanisms of photosensitized oxidation, Science, 162 (1968) 963–970. [PubMed: 4972417]

[43]. Foote CS, Definition of Type I and Type II photosensitized oxidation, Photochem. Photobiol 54 (1991) 659. [PubMed: 1798741]

[44]. Wilkinson F, Rate constants for the decay and reactions of the lowest electronically excited singlet state of molecular oxygen in solution: an expanded and revised compilation, J. Phys. Chem Ref. Data, 24 (1995) 663, 10.1063/1.555965.

[45]. Spikes JD, Photosensitization, in Smith KC (ed.) The Science of Photobiology, Plenum Press, New York, 1989, pp. 79–110.

[46]. Xue LY, Chiu SM, Oleinick NL, Photochemical destruction of the Bcl-2 oncoprotein during photodynamic therapy with the phthalocyanine photosensitizer Pc 4. Oncogene 20 (2001) 3420–3427. [PubMed: 11423992]

[47]. Brazil DP, Hemmings BA, Ten years of protein kinase signaling: a hard Akt to follow, Trends Biochem. Sci 26 (2001) 657–664. [PubMed: 11701324]

[48]. Vivanco I, Sawyers CL, The phosphatidylinositol 3-kinase/Akt pathway in human cancer, Nat. Rev. Cancer 2 (2002) 489–501. [PubMed: 12094235]

[49]. Hawkins PT, Anderson KE, Davidson K, Stephens LR, Signaling through Class I PI3Ks in mammalian cells, Biochem. Soc. Trans (2006) 647–662. [PubMed: 17052169]

[50]. Yuan TL, Cantley LC, PI3K pathway alterations in cancer: variations on a theme, Oncogene 27 (2008) 5497–5510. [PubMed: 18794884]

[51]. Toker A, Marmiroli S, Signaling specificity in the Akt pathway in biology and disease, Adv. Biol. Regul 55 (2014) 28–38. [PubMed: 24794538]

[52]. Myers MP, Pass I, Batty IH, Van der Kaay J, Stolarov JP, Hemmings BA, et al., The lipid phosphatase activity of PTEN is critical for its tumor suppressor function, Proc. Natl. Acad. Sci. USA, 95 (1998) 13513–13518. [PubMed: 9811831]

[53]. Cantley LC, Neel BG, New insights into tumor suppression: PTEN suppresses tumor formation by restraining the phosphoinositide 3-kinase/Akt pathway, Proc. Natl. Acad. Sci. USA, 96 (1999) 4240–4245. [PubMed: 10200246]

[54]. Leslie NR, Bennett D, Lindsay YE, Stewart H, Gray A, Downes CP, Redox regulation of PI3-kinase signaling via inactivation of PTEN, EMBO J, 22 (2003) 5501–5510. [PubMed: 14532122]

[55]. Lee SR, Yang KS, Kwon J, Lee C, Jeong W, Rhee SG, Reversible inactivation of the tumor suppressor PTEN by H_2O_2, J. Biol. Chem 277 (2002) 20336–20342. [PubMed: 11916965]

[56]. Girotti AW, Translocation as a means of disseminating lipid hydroperoxide-induced oxidative damage and effector action, Free Radic Biol Med 44 (2008) 956–968. [PubMed: 18206663]

[57]. Goodman RH, Smolik S, CBP/p300 in cell growth, transformation, and development, Genes Dev. 14 (2000) 1553–1577. [PubMed: 10887150]

[58]. Shikama N, Lyon J, La Thangue NB, The p300/CBP family: integrating signals with transcription factors and chromatin, Trends Cell. Biol 7 (1997) 230–236. [PubMed: 17708951]

[59]. Chen LF, Mu Y, Greene WC, Acetylation of RelA at discrete sites regulates distinct nuclear functions of NF-κB, EMBO J, 21 (2002) 6539–6548. [PubMed: 12456660]

[60]. Wang F, Marshall CB, Ikura M, Transcriptional/epigenetic regularor CBP/p300 in tumorigenesis: structural and functional versatility in target recognition, Cell. Mol. Life Sci 70 (2013) 3989–4008. [PubMed: 23307074]

[61]. Huang B, Yang XD, Zhow MM, Ozato K, Chen LF, Brd4 coactivates transcriptional activation of NF-κB via specific binding of acetylated RelA, Mol. Cell. Biol 29 (2009) 1375–1387. [PubMed: 19103749]

[62]. Zou Z, Huang B, Wu X, Zhang H, Qi J, Bradner J, et al., Brd4 maintains constitutively active NF-κB in cancer cells by binding to acetylated RelA, Oncogene 33 (2014) 2395–2404. [PubMed: 23686307]

[63]. Huang WC, Chen CC, Akt phosphorylation of p300 at Ser-1834 is essential for its histone acetyltransferase and transcriptional activity, Mol. Cell. Biol 25 (2005) 6592–6602. [PubMed: 16024795]

[64]. Kleszcz R, Paluszczak J, Baer-Dubowska W, Targeting aberrant cancer metabolism - The role of sirtuins. Pharmacol Rep. 67 (2015) 1068–1080. [PubMed: 26481524]

[65]. Lin Z, Fang D, The roles of SIRT1 in cancer, Genes Cancer, 4 (2013) 97–104. [PubMed: 24020000]

[66]. Kauppinen A, Suuronen T, Ojala J, Kaarniranta K, Salminen A, Antagonistic crosstalk between NF-κB and SIRT1 in the regulation of inflammation and metabolic disorders, Cell Signal., 25 (2013) 1939–1948. [PubMed: 23770291]

[67]. Yeung F, Hoberg JE, Ramsey CS, Keller MD, Jones DR, Frye RA, et al., Modulation of NF-kappa B-dependent transcription and cell survival by the SIRT1 deacetylase. EMBO J. 23 (2004) 2369–2380. [PubMed: 15152190]

[68]. Zhuang T, Chelluboina B, Ponnala S, Velpula KK, Rehman AA, Chetty C et al. Involvement of nitric oxide synthase in matrix metalloproteinase-9- and/or urokinase plasminogen activator receptor-mediated glioma cell migration. BMC Cancer, 13 (2013) 590. [PubMed: 24325546]

[69]. Palumbo P, Lombardi F, Siragusa G, Dehcordi SR, Luzzi S, Cimini A, et al. Involvement of NOS2 activity on human glioma cell growth, clonogenic potential, and neurosphere generation. Int. J. Mol. Sci 19 (2018) pii: E2801. doi: 10.3390/ijms19092801. [PubMed: 30227679]

[70]. Ribas V, García-Ruiz C, Fernández-Checa JC, Mitochondria, cholesterol and cancer cell metabolism, Clin. Transl. Med 5 (2016) 22. doi: 10.1186/s40169-016-0106-5. [PubMed: 27455839]

[71]. Tsai YJ, Tsai T, Peng PC, Li PT, Chen CT, Histone acetyltransferase p300 is induced by p38MAPK after photodynamic therapy: the therapeutic response is increased by the p300HAT inhibitor anacardic acid. Free Radic. Biol. Med 86 (2015) 118–132. [PubMed: 26001729]

[72]. Bazak J, Fahey JM, Wawak K, Korytowski W, Girotti AW, Enhanced aggressiveness of bystander cells in an anti-tumor photodynamic therapy model: Role of nitric oxide produced by targeted cells. Free Radic. Biol. Med, 102 (2017) 111–121. [PubMed: 27884704]

[73]. Tetard MC, Vermandel M, Mordon S, Lejeune JP, Reyns N, Experimental use of photodynamic therapy in high grade gliomas: a review focused on 5-aminolevulinic acid, Photodiagnosis Photodyn. Ther 11 (2014) 319–330. [PubMed: 24905843]

- 5-Aminolevulinic acid (ALA)-based photodynamic therapy (PDT) is a promising treatment for glioblastoma.
- ALA-PDT generates the cytotoxic ROS singlet oxygen ($^1O_2$).
- $^1O_2$ activates a PI3K/Akt/p300/p65-acK resistance network.
- Lysine deacetylase Sirt1 is concurrently downregulated.
- A major outcome of these events is upregulation of pro-survival/expansion iNOS/NO.

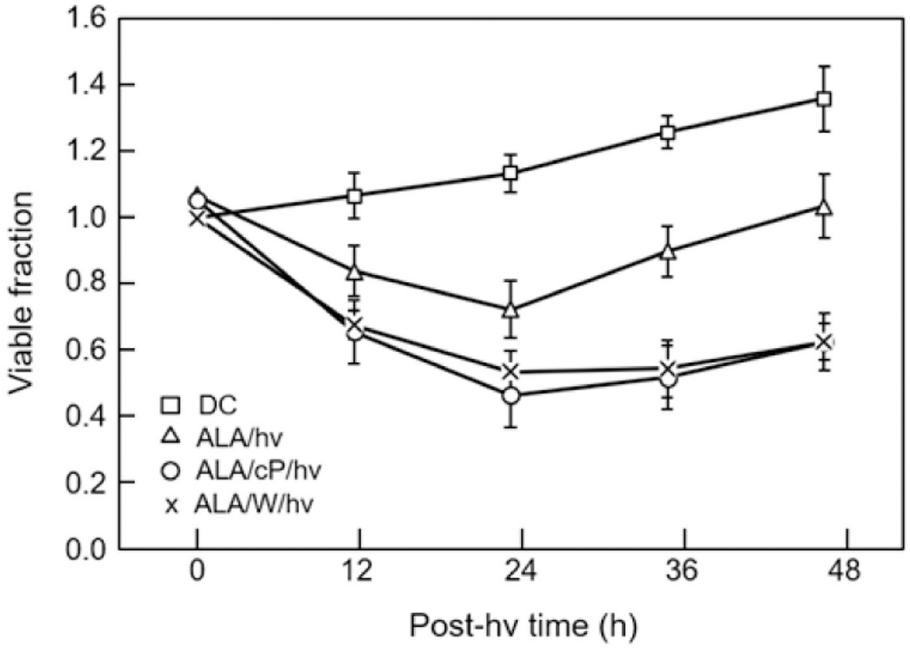

Fig. 1.

Cytoprotective and growth-stimulatory effects of endogenous iNOS/NO in PDT-challenged U87 cells. Cells at ~65% confluence in 35-mm dishes were pre-incubated with ALA (1 mM, 30 min), and then irradiated (1 J/cm^2) in the absence *vs.* presence of 1400W (50 μM) or cPTIO (50 μM). The viable cell fraction was then determined over 24 h of post-irradiation incubation, using the CCK-8 assay. At 24 h post-hv, some cultures were washed and proliferation of remaining live cells in 10% FBS-medium −/+ 1400W or cPTIO was tracked over an additional 24 h. Plotted values are means ± SE (n=3).

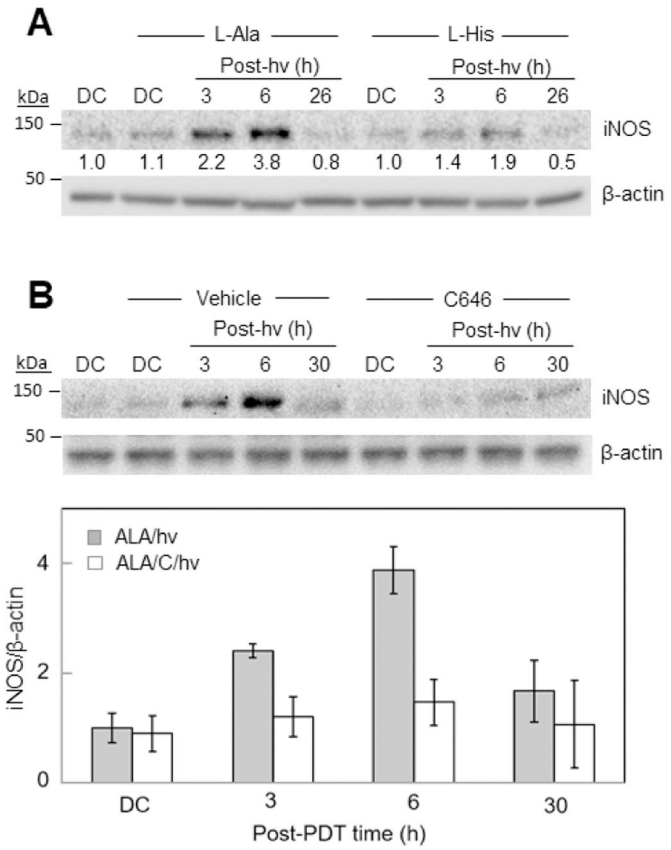

Fig. 2.

Inhibitory effects of a $^1O_2$ scavenger and a p300 inhibitor on post-PDT iNOS upregulation in U87 cells. (A) ALA-treated cells were irradiated in the absence *vs.* presence of 3 mM L-His or 3 mM L-Ala. At the indicated post-hv times, cell samples were recovered for Western blot analysis of iNOS levels; total protein per lane: 100 μg. ALA-treated dark controls (DC) were run alongside. Numbers below bands represent iNOS band intensity relative to β-actin and normalized to DC. (B) ALA-treated cells were irradiated in the absence *vs.* presence of 25 μM C646 or DMSO (vehicle control), then recovered for Western blot analysis of iNOS at the indicated post-hv times. One blot from three replicate experiments is shown and band intensities are plotted as means ± SEM (n=3); *P<0.01 *vs.* ALA/hv.

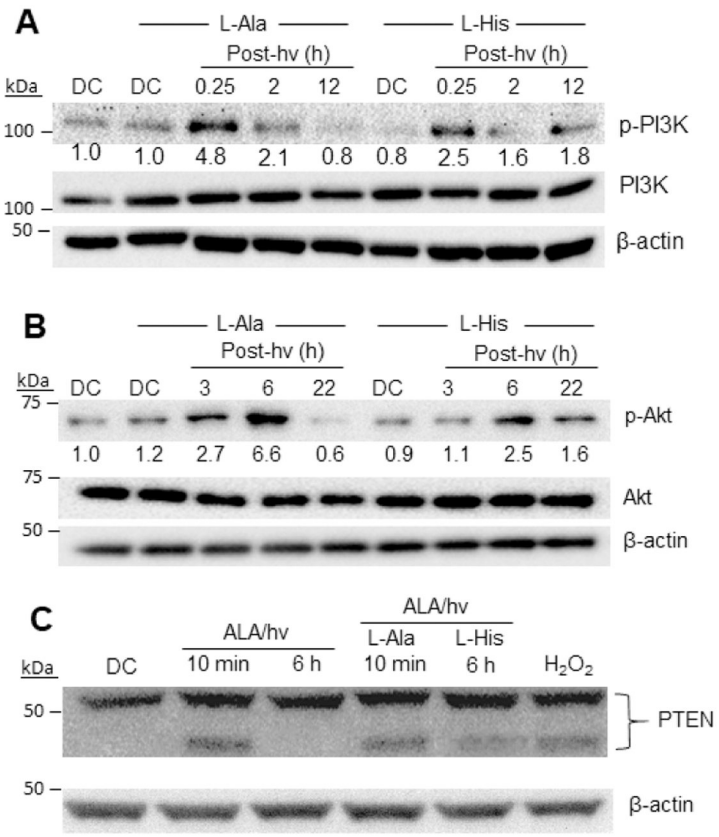

Fig. 3.

Role of $^1O_2$ in phosphorylation-activation of PI3K/Akt and disulfide-inactivation of PTEN in U87 cells. ALA-treated cells were either not irradiated (DC) or irradiated (1 J/cm^2) in the presence of 3 mM L-His or 3 mM L-Ala. After the indicated post-hv incubation times, samples were recovered for Western blot analyses of (A) p-PI3K (p-Tyr199/458) and total pI3K; (B) p-Akt (p-Ser-473) and total Akt; and (C) PTEN. Reducing conditions were used in (A) and (B), and non-reducing conditions in (C). The PTEN blot also shows the effects of H_2O_2 treatment (0.25 mM for 2 h).

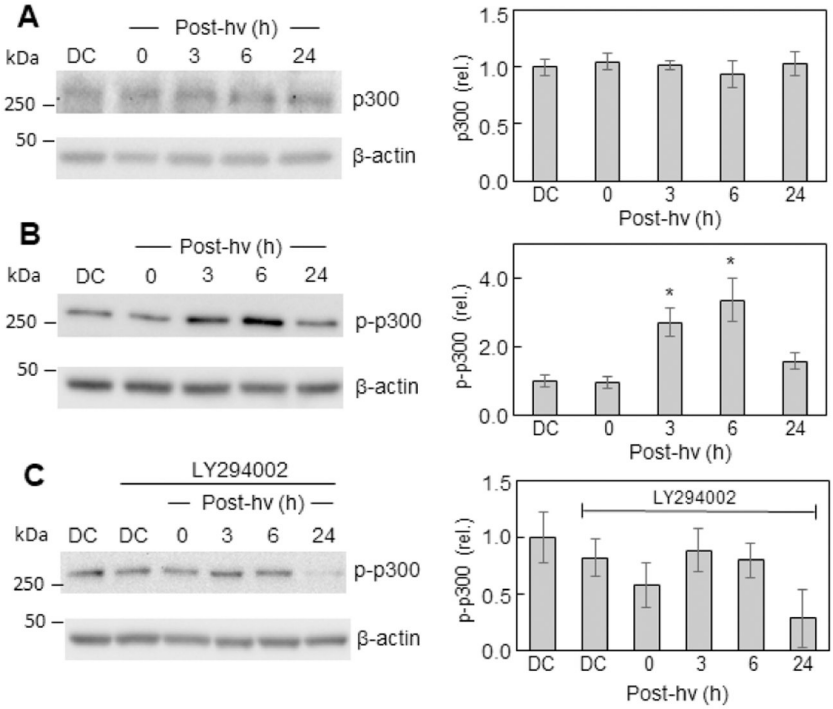

Fig. 4.

Total p300 and phospho-p300 levels before and after PDT: effects of a PI3K inhibitor. After pre-incubation with ALA, U87 cells were irradiated as described in Fig. 1. After the indicated periods of post-PDT incubation, cell samples were analyzed for total protein concentration, then subjected to Western blot analysis, using an antibody for overall p300 (A) or an antibody for p-p-300 (p-Ser-1834) (B). Other cells were treated with the PI3K inhibitor LY294002 (20 μM) immediately after irradiation, then checked for p-p300 levels at the indicated times (C). Dark controls (DC) −/+ LY294002 were analyzed as well. Total protein load per lane: 100 μg (A, B, C). Each immunoblot is a representative one from three replicate experiments; in each case, band intensities relative to β-actin and normalized to DC are plotted as means ± SEM (n=3); *P<0.01 *vs.* DC (plot B).

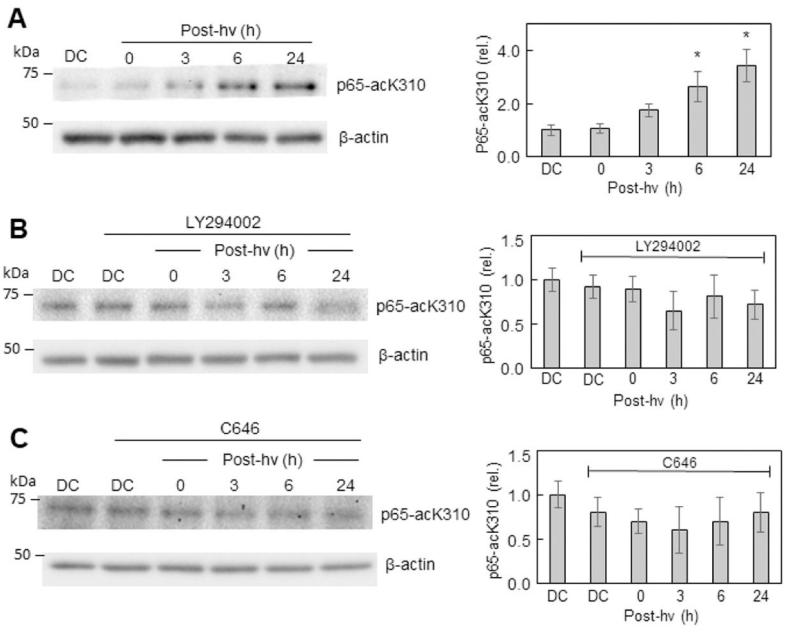

Fig. 5.

Upregulation of p65-acK310 after a PDT challenge and mitigation thereof by a PI3K inhibitor or p300 inhibitor. (A) ALA-treated U87 cells were irradiated (*cf.* Fig. 1) and at the indicated post-hv times, probed for acetylated lysine-310 levels by immunoblotting, using an antibody against p65-acK310. Similarly, sensitized cells were treated with (B) LY294002 (20 μM) or (C) C646 (25 μM) immediately after irradiation and analyzed for p65-acK310 levels by Western blotting at the indicated post-hv times, along with appropriate dark controls. Each blot is representative of three replicate experiments, and the accompanying plot shows normalized relative band intensities as means ± SEM (n=3); *P<0.05 *vs.* DC (plot A).

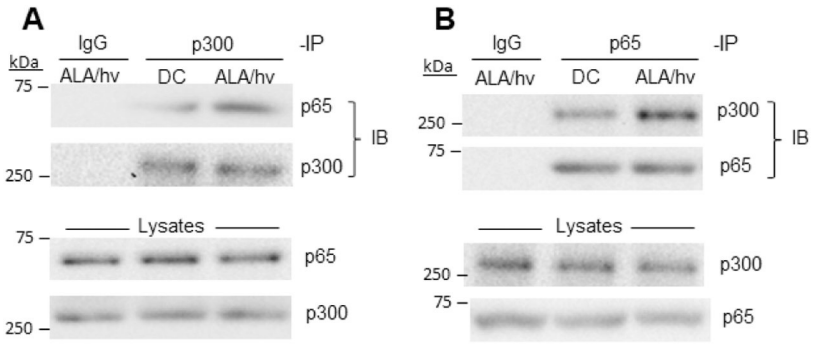

Fig. 6.

PDT-stimulated binding of p300 to p65. U87 cells were sensitized with ALA-induced PpIX and irradiated using a light fluence of ~1 J/cm^2. After 6 h of dark incubation, irradiated cells and dark controls (DC) were lysed, checked for total protein concentration, then subjected to immunoprecipitation (IP) steps, using a monoclonal antibody against p300 (A) or p65 (B). After 16 h of incubation with either antibody at 4 °C, followed by 6 h with protein A-conjugated Sepharose beads, bound proteins were eluted and subjected to immunoblotting (IB), using a monoclonal antibody against (A) p65 or p300 or (B) p300 or p65. Non-specific IgG was used as a control. Also shown are IB-detected p65 and p300 levels in total lysates.

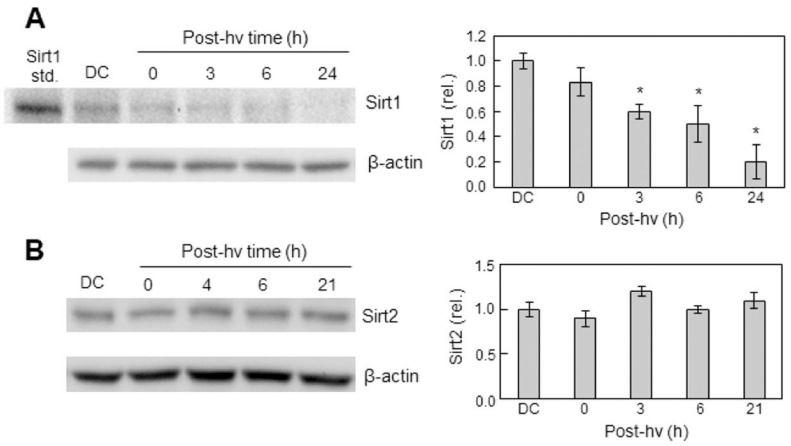

Fig. 7.

Effects of PDT on Sirt1 *versus* Sirt2 levels in U87 cells. U87 cells were exposed to ALA/light or ALA alone (DC) under conditions defined in Fig. 1. After the indicated post-irradiation times or 24 h for DC, samples were recovered for immunoblotting of Sirt1 (A) and Sirt2 (B). In (A), a sample of human recombinant Sirt1 was run alongside as a standard. For each analyte, a representative Western blot for an experiment run in triplicate is shown, along with a plot of band intensities relative to β-actin and normalized to DC; means ± SEM (n=3); *P<0.01 *vs.* DC (plot A).

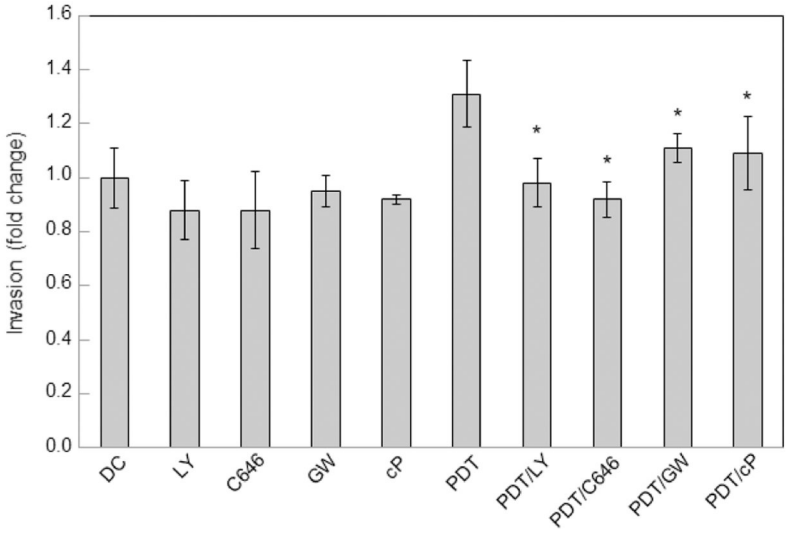

Fig. 8.

Increased invasiveness of PDT-surviving cells: mitigation by a PI3K inhibitor, p300 inhibitor, or iNOS/NO inhibitor. PDT-challenged U87 cells, along with non-irradiated controls (DC), were harvested into serum-free medium lacking or containing the following inhibitors: LY294002 (LY, 20 μM), C646 (50 μM), GW274150 (GW, 75 μM)), or cPTIO (cP, 50 μM). The cells were transferred to the upper wells of a 96-place trans-well device and allowed to invade through Matrigel-infused filters toward 10% FBS-containing medium in the lower wells. After 24 h in the incubator, cells adhering to the filter undersides were centrifuged off into the lower wells and quantified in terms of live cell counts. Plotted data are means ± SD of values from 5 separate experiments; *P<0.01 *vs.* DC; **P<0.01 *vs.* PDT; #P<0.05 *vs.* PDT.

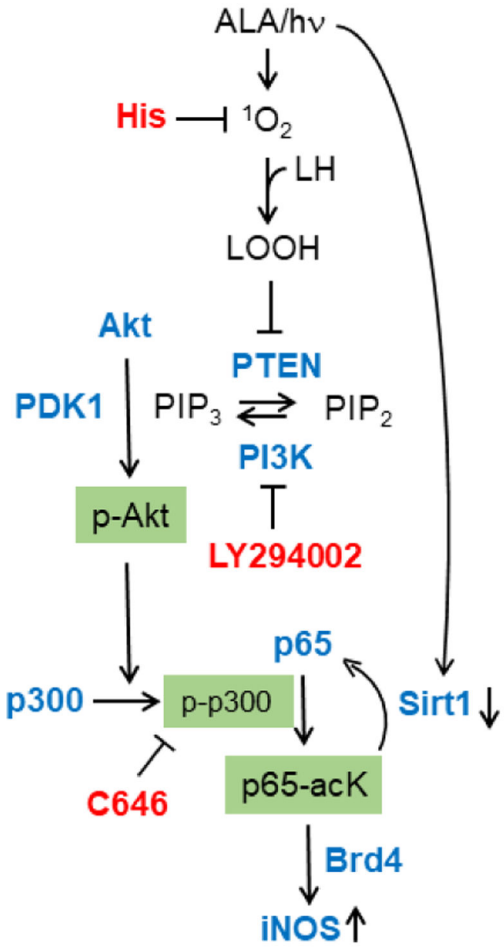

Fig. 9.

Scheme depicting PDT-provoked signaling events leading to iNOS induction. Key effector proteins (Akt, PI3K, p300, p65) are shown along with targets of the inhibitors used (L-His, LY294002, C646).